Self-Assembled Structure of the Binary Complex of DNA with Cationic Lipid

Ching-Mao Wu,[†] Willisa Liou,[‡] Hsin-Lung Chen,*[,†] Tsang-Lang Lin,[§] and U-Ser Jeng[⊥]

Department of Chemical Engineering, National Tsing Hua University, Hsin-Chu, Taiwan 30013, R.O.C.; Department of Anatomy, Chang Gung University, Kwei-San, Taoyuan, 333, Taiwan, R.O.C.; Department of Engineering and System Science, National Tsing Hua University, Hsin-Chu, Taiwan 30013, R.O.C.; and National Synchrotron Radiation Research Center, Hsin-Chu, Taiwan 300, R.O.C.

Received March 7, 2004; Revised Manuscript Received May 3, 2004

ABSTRACT: Polyanionic DNA can bind electrostatically with cationic lipid to form the complex exhibiting rich self-assembled structures at various length scales. This class of bioassembly has been considered as a nonviral gene delivery system for gene therapy and as a template for nanostructure construction. The present study reports the self-assembled structure of the binary complex of DNA with a cationic lipid, cholesteryl 3β-*N*-((dimethylamino)ethyl)carbamate (DC-Chol), in the presence of excess water. Neat DC-Chol self-assembled into cylindrical micelles in aqueous media. These micelles aggregated and fused into multilamellar condensates or vesicles upon complexation with DNA, and the DNA chains confined between the lipid bilayers formed closely packed arrays irrespective of the overall lipid-to-base pair molar ratio. The complexation was found to be a highly cooperative process, where the complexes with nearly 1:1 stoichiometry were formed even when DNA was in excess of DC-Chol in terms of the overall ionic charge. As DC-Chol became in excess, the unbound lipids did not fully macrophase separate from the stoichiometric complex but segregated to form domains coexisting with the bound lipid domains in the lamellae. The presence of these unbound lipid domains reduced the persistence length of the membrane and consequently induced topological transformation of the multilamellar phase from platelike lamellae to circular lamellae observed by TEM at higher DC-Chol composition.

Introduction

Complexes of polyelectrolyte with oppositely charged surfactants or lipids constitute a new class of material that combines the surfactant/lipid mesophase with the functions or properties of the polymer.[1−3] The driving force of the complexation is the electrostatic attraction between the ionic charges on the polymer and the oppositely charged headgroup of the surfactant/lipid micellar species coupled with the entropic gain from counterion release. Among the variety of the complex systems, the complexes of polyanionic DNA with cationic liposomes have drawn much attention recently because of their application as nonviral gene vector for gene therapy.[4−7] Cationic liposomes are vesicles with aqueous volume entirely enclosed by a bilayer membrane composed of cationic lipids. For gene delivery application the liposomes are commonly formed by mixing a synthetic cationic lipid with a zwitterionic phospholipid.[8,9] The zwitterionic lipid is added to enhance the liposome's compatibility with cell membrane and to regulate the membrane spontaneous curvature so as to facilitate the bilayer formation in the case where the cationic lipid alone is unable to form such a structure.[10]

Besides their application in gene delivery, DNA/cationic liposome complexes may also be considered as templates for nanostructure construction in light of their rich self-assembled structures.[4,8,9,11−28] The predominant structure observed is a multilamellar phase with alternating lipid bilayer and DNA monolayer (denoted by L_α^C phase).[4,8,13,14] The DNA chains confined between the lipid bilayers adopt a smectic order, giving rise to a DNA−DNA correlation peak in the X-ray scattering profile.[4,8] In addition to L_α^C phase, an inverted hexagonal columnar phase (denoted by H_{II}^C phase) with DNA contained within lipid tubes has been constructed through reduction of the membrane bending rigidity by adding low-molecular-weight helper molecules or induction of negative spontaneous membrane curvature by adding a zwitterionic lipid with conelike molecular shape.[15] Both L_α^C and H_{II}^C phases yield ordered DNA arrays, and through binding inorganic substances on the DNA chains,[29] for instance, these structures serve as the templates to produce spatially ordered nanowires.

Driven by the abundant interests in gene delivery application, studies of DNA/cationic liposome complexes have been focusing almost exclusively on the ternary systems in which the liposomes consist of a cationic lipid and a zwitterionic lipid component. In this case, the zwitterionic lipid is regarded as an inert species toward DNA binding, and its presence in the membrane homogeneously swells the interhelical distance of DNA. For application as nanostructure templates, the complexes consisting of a single cationic lipid component, whose structure remains largely unexplored, would also be of interest. The objective of this study is to examine the self-assembled structure of the binary complex system as a function of composition to reveal the structures induced without the intervention of zwitterionic lipid. The cationic lipid chosen for the study is cholesteryl 3β-*N*-((dimethylamino)ethyl)carbamate (DC-Chol), which has been described as a promising gene vector system

[†] Department of Chemical Engineering, National Tsing Hua University.
[‡] Chang Gung University.
[§] Department of Engineering and System Science, National Tsing Hua University.
[⊥] National Synchrotron Radiation Research Center.

10.1021/ma049541p CCC: $27.50
Published on Web 06/02/2004

with the following chemical structure:[30]

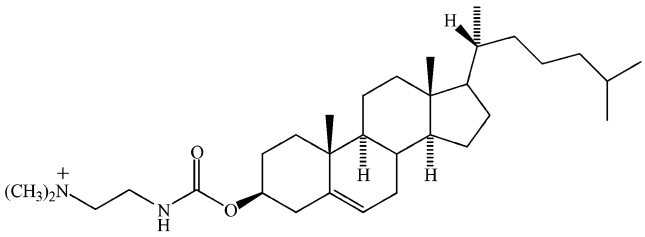

Unlike the typical lipids carrying two alkyl tails per molecule to render sufficient hydrocarbon volume for bilayer formation, it will be shown here that DC-Chol molecules self-assemble into wormlike micelles in aqueous media. For gene therapy application, this lipid was usually mixed with a zwitterionic lipid to form liposome prior to DNA complexation.[7,30] In this study, it will be shown that despite the absence of bilayer entities for neat DC-Chol, the subsequent complexation with DNA induces formation and ordering of bilayers, where the DC-Chol micelles transform into a multilamellar structure after the complexation. The interhelical distance between the DNA chains confined between the fully cationic bilayers and the topological structures of the multilamellar phase observed by transmission electron microscopy (TEM) will also be discussed.

Experimental Section

Materials and Complex Preparations. Linear DNA-type XIV from herring testes sodium salt (Na content 6.2%, H_2O content 4.5%) was purchased from Sigma and used without further purification. Its molecular weight determined by gel electrophoresis was found to have a polydisperse value between 400 and 1000 base pairs (bp) with a center of distribution at ca. 700 bp.[31] The cationic lipid, DC-Chol, was also obtained from Sigma.

For the complex preparation, the DC-Chol lipid was first dissolved in choloform followed by drying in vacuo at room temperature to form a lipid film. The lipid film was hydrated by adding distilled water, mixing with a vortex mixer for several minutes, and then sonicating in a water bath at 40 °C. The concentration of the resultant DC-Chol suspension was 3−6 wt % depending on the compositions of the complexes to be prepared. DNA/DC-Chol complexes were prepared by adding prescribed amounts of 50 mg/mL DNA aqueous solutions into DC-Chol suspensions, and the complexes formed spontaneously as manifested by their precipitation. The concentration of the complexes in the aqueous media was 5 wt % (or water content = 95 wt %).

Ultraviolet−Visible (UV−Vis) Spectroscopy Experiment. UV−vis spectroscopy (Hitachi U-3300 spectrophotometer) was employed to determine the actual compositions of the complexes prepared when DNA was in excess of DC-Chol in terms of overall ionic charge by measuring the concentrations of free DNA remained in the supernatants. The separation between the supernatant and the complex precipitate was facilitated by centrifugation. Each milliliter of the supernatant was subsequently diluted with 14 mL of deionized water to reduce the intensity of the DNA absorption peak near 260 nm to the detectable range of the spectrophotometer.

Small-Angle X-ray Scattering (SAXS) Measurements. The self-assembled structures of the DNA/DC-Chol complexes in excess water were probed by SAXS at room temperature. The samples were prepared by directly introducing the aqueous suspensions into the sample cells comprising of two Kapton windows. The SAXS apparatus consisted of an 18 kW rotating anode X-ray generator (Rigaku) operated at 200 mA and 40 kV, a pyrotic graphite crystal for incident beam monochromatization, and a two-dimensional position-sensitive detector (ORDELA model 2201X, Oak Ridge Detector Laboratory Inc.) with 256 × 256 channels (active area 20 × 20 cm^2 with ∼1 mm resolution). The background (dark current and empty beam scattering) and the sensitivity of each pixel of the area detector were corrected for all the data. The area scattering pattern was radially averaged to increase the efficiency of data collection. The intensity profile was output as the plot of the scattering intensity (I) vs the scattering vector, $q = 4\pi/\lambda \sin(\theta/2)$ (θ = scattering angle). All the intensity profiles reported here have also been corrected for thermal diffuse scattering (TDS). TDS was considered as a positive deviation from Porod's law and may be associated with thermal motion, local disorder, or onset of wide-angle scattering region. The intensity level of TDS was assumed to be a constant, and its magnitude was determined from the slope of the Iq^4 vs q^4 plot at the high-q region.[32]

Transmission Electron Microscopy (TEM) Experiment. TEM was utilized to examine the real-space morphology of DNA/DC-Chol complexes. The specimens were prepared by a negative staining method which effectively vitrified the structure in the excess water state.[33] A 5 μL drop of the aqueous suspension was deposited onto a copper grid bearing a carbon-coated Formvar film. The solution was allowed to stand for 1 min and then withdrawn with the tip of a piece of filter paper until a very thin layer of fluid formed on the grid surface. The samples were immediately stained for 1 min with 4% acidic uranyl acetate aqueous solution and for another minute in a methycellulose/uranyl acetate mixture (1.8%/0.3%). The ultrathin specimens were then examined by a JEOL 2000EXII TEM operated at 100 kV.

Results and Discussion

The composition of the complex denoted by "x" represents the lipid-to-base pair molar ratio prescribed by the feed ratio of DNA and DC-Chol in the complex preparation (x is thus called "prescribed composition" here). Because each DC-Chol molecule has a positive charge and a base pair of DNA carries two negative charges, $x = 2.0$ corresponds to the overall stoichiometric composition for charge neutralization. $x < 2$ means DNA is in excess of the lipid in terms of overall ionic charge, while the opposite is true for $x > 2$. The actual composition of the complex, denoted by "x_a", may however deviate from the prescribed composition. x_a should correspond to 1:1 stoichiometry (i.e., $x_a = 2$) for the system with $x > 2$ because there is a sufficient supply of lipid molecules for binding with all DNA phosphates groups in the system. In this case, the stoichiometric complex coexists with free lipids in the aqueous media. The situation becomes more complicated for $x < 2$ where the supply of lipid molecules is not enough for complete binding. Intuitively, the lipid molecules might be allocated evenly to all DNA chains in the system according to the feed ratio. However, the complexation of polyelectrolyte with oppositely charged surfactant is known to be a highly cooperative process, where the surfactant binding neighboring a "docked" surfactant molecule is much faster than the primary binding.[34−38] Such a "zipper" binding mechanism tends to yield 1:1 stoichiometry for the complex composition even when the polyelectrolyte is in excess of the surfactant in terms of the overall ionic charge. In this case, the system contains the stoichiometric complex (which precipitated out of the solution) along with free polyelectrolyte remained in the supernatant.

To examine whether the cooperative binding is operative in the complexation between DNA and DC-Chol, the actual compositions of the complexes formed at $x <$ 2 were determined by measuring the concentrations of free DNA remained in the supernatants using UV−vis spectroscopy. Figure 1a displays the representative UV

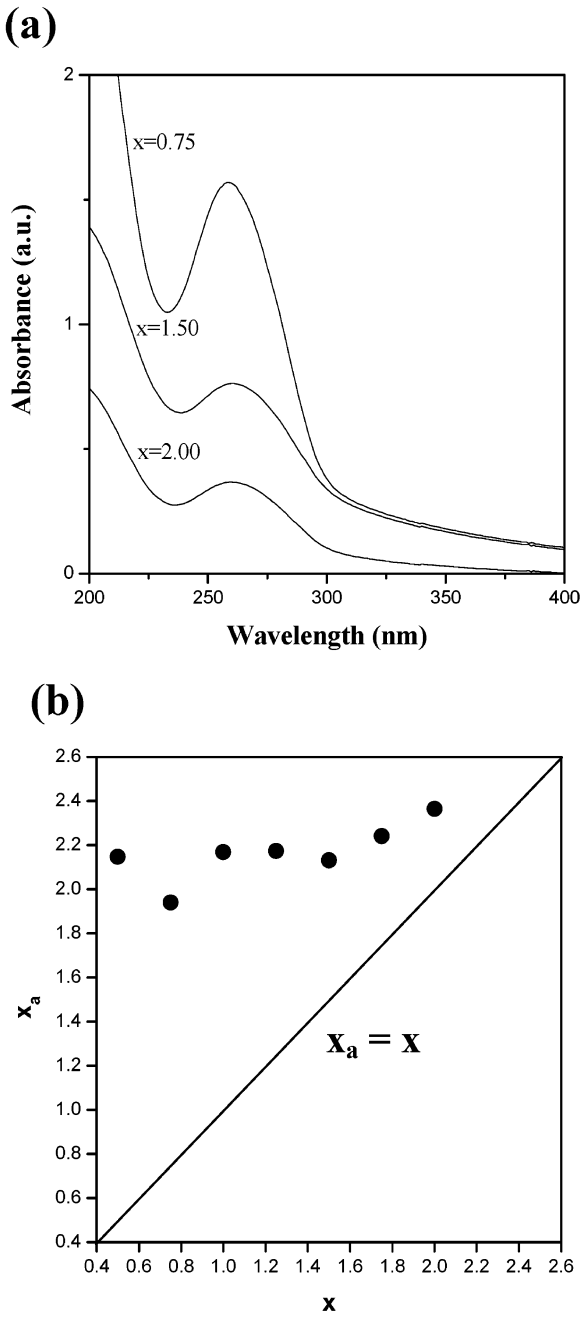

Figure 1. (a) Representative UV spectra of the supernatants for the samples with $x = 0.75$, 1.5, and 2.0. The existence of free DNA is clearly demonstrated by the DNA absorption peak near 260 nm. (b) The actual complex composition x_a obtained from eq 1 vs the corresponding prescribed composition. It can be seen that x_a is about 2.2 irrespective of x.

spectra of the supernatants for the samples with $x = 0.75$, 1.5, and 2.0. The existence of free DNA is clearly demonstrated by the DNA absorption peak near 260 nm. The intensity of this peak increases with decreasing x, indicating that the concentration of DNA participating in the complexation with DC-Chol decreases accordingly. The concentration of free DNA in the supernatant, c_{DNA}^{s}, in units of mg/mL can be determined from the peak absorbance; the actual complex composition is then given by

$$x_a = x\left(\frac{c_{DNA}^{0}}{c_{DNA}^{0} - c_{DNA}^{s}}\right) \quad (1)$$

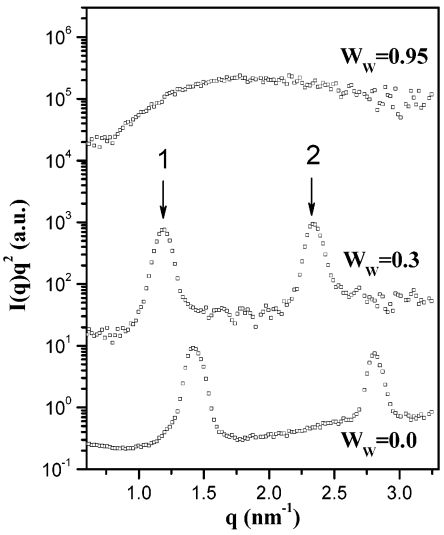

Figure 2. Lorentz-corrected SAXS profiles of neat DC-Chol as a function of weight fraction of water (W_w).

where c_{DNA}^{0} is the total DNA concentration in the system. x_a obtained from eq 1 is plotted against the corresponding prescribed composition in Figure 1b. It can be seen that x_a is about 2.2 irrespective of x. The proximity of x_a to the value of 2.0 asserts that the complexation is indeed highly cooperative, where the binding of DC-Chol molecules onto DNA proceeds through a zipper mechanism. Although the prescribed composition does not correctly represent the actual complex composition, the overall lipid-to-base pair molar ratio is still a key parameter governing the structures of the complexes, as will be demonstrated later. Consequently, the following results relating to the complex structures will be presented in terms of x rather than x_a for the clarity of discussion.

The self-assembled structures of the complexes are probed by SAXS. Figure 2 displays the Lorentz-corrected SAXS profiles ($I(q)q^2$ vs q) of neat DC-Chol as a function of water content (W_w = weight fraction of water). Dry DC-Chol exhibits a multilamellar structure as manifested by the multiple scattering peaks with relative positions prescribed by the 1-D stacked lamellar morphology (i.e., 1: 2...). The interlamellar distance of 4.42 nm signifies that the membrane is in the bilayer form as the fully extended length of a DC-Chol molecule is ca. 2.0 nm. Absorption of water swells the interlamellar distance (to 5.23 nm for $W_w = 0.3$) due to the incorporation of water molecules into the hydrophilic layers to reduce the electrostatic repulsion between the bilayer surfaces. For the excess water state ($W_w = 0.95$) concerned here, the multiple diffraction peaks are replaced by a broad halo, signaling that the lamellar order has been completely lost.

Figure 3 shows the TEM micrograph of neat DC-Chol. DC-Chol is seen to form wormlike cylindrical micelles rather than unilamellar or multilamellar vesicles, consistent with the SAXS result showing no multilamellar peaks at high water content. The diameter of the micelles estimated from the micrograph is about 5.4 nm. It is known that the type of micelle formed is governed by the geometric factor, $v/l_c a_0$, of the lipid molecule with v, l_c, and a_0 being the hydrocarbon volume, critical length of the lipid chain, and the effective headgroup area, respectively.[39] Planar bilayer is favored for $v/l_c a_0 > 1/2$, while smaller $v/l_c a_0$ favors the formation of micelles with higher surface curvature such as cylinders

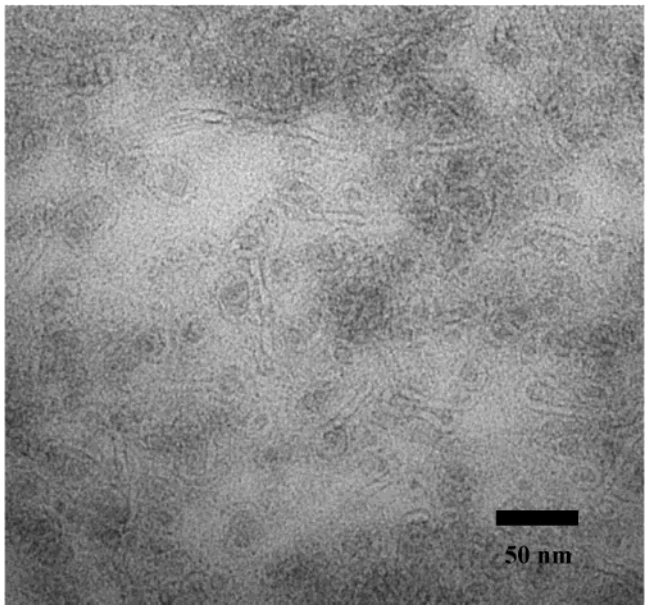

Figure 3. TEM micrograph of neat DC-Chol showing the formation of wormlike cylindrical micelles with the diameter of ca. 5.4 nm.

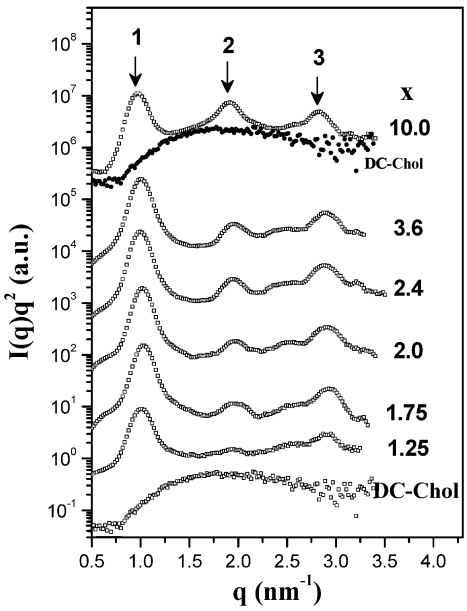

Figure 4. Representative Lorentz-corrected SAXS profiles of DNA/DC-Chol complexes in excess water. For $x = 10.0$ the multilamellar peaks in the corresponding SAXS profile appear to superpose on a broad halo (represented by the legend of filled circle) due to the presence of unbound DC-Chol micelles.

or spheres. The molecule of DC-Chol is truncated cone in shape when the effective headgroup area is swollen by sufficient hydration; in this case, the corresponding value of $v/l_c a_0$ lies between $^1/_2$ and $^1/_3$ and hence favors the formation of cylindrical micelles. Dehydration of the headgroup by reducing water content decreases a_0 such that bilayer becomes the stable structure.

Figure 4 presents the Lorentz-corrected SAXS profiles of DNA/DC-Chol complexes in excess water. In contrast to neat DC-Chol, all the complexes are found to exhibit the multilamellar structure characterized by an interlamellar distance of 6.28 nm irrespective of the prescribed composition. Consequently, complexation with DNA induces both formation and ordering of DC-Chol bilayers (without the assistance of the zwitterionic helper lipid) as the electrostatic interaction with DNA effectively dehydrates the headgroups of DC-Chol. It is noted that, at $x = 10.0$ where the molar number of the lipid greatly exceeds that of the base pairs, the multilamellar peaks in the corresponding SAXS profile appear to superpose on a broad halo, implying that the multilamellar structure coexists with the uncomplexed DC-Chol micelles.

The multilamellar phases in the complexes are further verified by the TEM micrographs in Figure 5, showing the multilamellar structure in the complex particles. At $x = 10$, hallow multilamellar vesicles are observed along with the unbound DC-Chol micelle aggregates (marked by the arrow in Figure 5a). The coexistence of these two entities is consistent with the corresponding SAXS profile, showing a broad halo overlapped with the multilamellar peaks. At $x = 2.4$ and 3.6 large compact aggregates consisting of circular lamellae are predominantly found in the system. It is noted that although the lipid is in excess of DNA in these two compositions, no cylindrical micelle formed by free DC-Chol is observed. This suggests that the unbound DC-Chol molecules are somehow contained within the multilamellar particles rather than macrophase separating from them. When DNA becomes in excess of lipid in terms of overall charge (i.e., at $x < 2.0$), the stoichiometric complexes tend to form platelike lamellae with opened edges, as demonstrated in Figure 5d for $x = 0.5$. The TEM observation indicates that the multilamellar phases tend to exhibit a topological change from platelike lamellae to circular lamellae to multilamellar vesicles with increasing x.

Returning to the SAXS results, a close examination of the SAXS profiles of the complexes reveals the presence of a small peak marked by q_{DNA} situating at ca. 2.50 nm^{-1} for $1.25 \leq x \leq 3.6$, as demonstrated by the enlarged SAXS plots in Figure 6. This peak is attributed to the DNA−DNA correlation prescribed by the smectic order of the DNA chains confined in the hydrophilic layers.[4] The observed q_{DNA} corresponds to the interhelical distance of the DNA chains $d_{DNA} = 2\pi/q_{DNA} = 2.51$ nm. This length approaches the diameter of DNA plus a layer of hydration shell,[40] indicating that the DNA chains in the hydrophilic layers form closely packed arrays irrespective of the prescribed composition.

To gain further insight into the multilamellar structures at different x, the electron density profiles along the lamellar normal, $\rho_e(z)$, are constructed from the SAXS data via[41−43]

$$\rho_e(z) \sim \sum_{k=1}^{n} \sqrt{I(q_k){q_k}^2}\phi_k \cos(q_k z) \qquad (2)$$

where n is the total number of diffraction order, q_k is the scattering vector of the kth diffraction order, $[I(q_k)q_k^2]^{1/2}$ is the magnitude of the kth amplitude, and ϕ_k is phase which is either +1 or −1 for the centrosymmetical multilamellar structure.[41]

Figure 7 presents the relative electron density profiles of the complexes and neat DC-Chol with $W_w = 0.3$ calculated using the intensities of the three scattering peaks and the most reasonable phase combination of (−1, −1, −1) and (−1, −1, +1) for the complexes[43] and neat DC-Chol,[41,44] respectively. The overall shapes of $\rho_e(z)$ are seen to deviate from the two-density model commonly adopted for the analysis of multilamellar

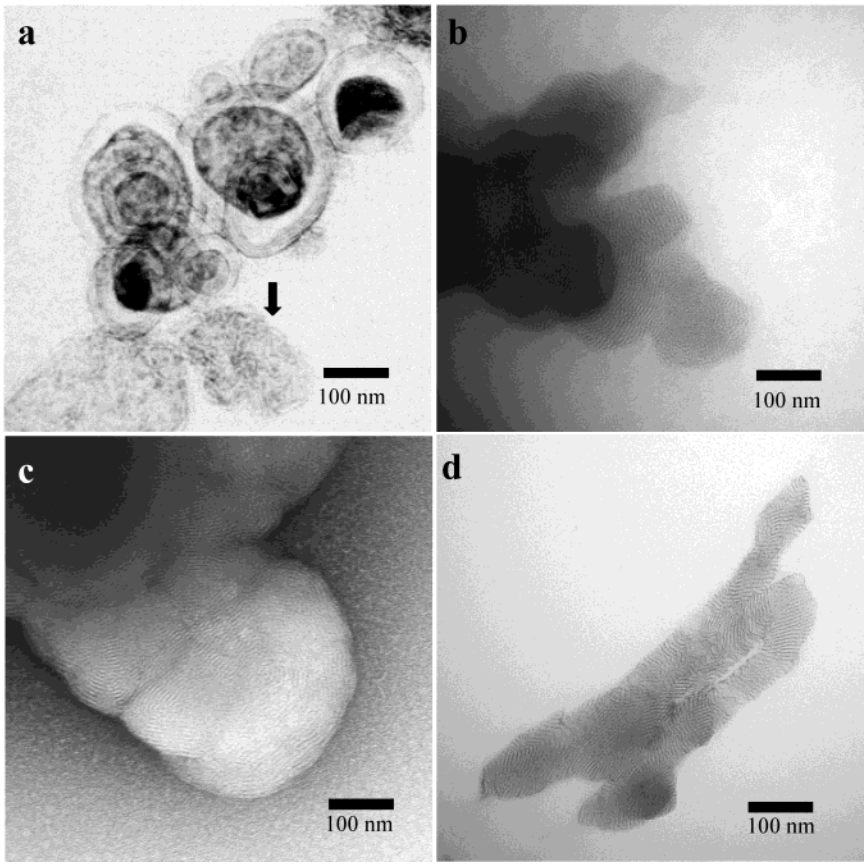

Figure 5. A series of TEM micrographs showing the multilamellar phases of DNA/DC-Chol complexes: (a) $x = 10.0$; (b) $x = 3.6$; (c) $x = 2.4$; (d) $x = 0.5$. In (a) the arrow marks the presence of unbound DC-Chol micelles.

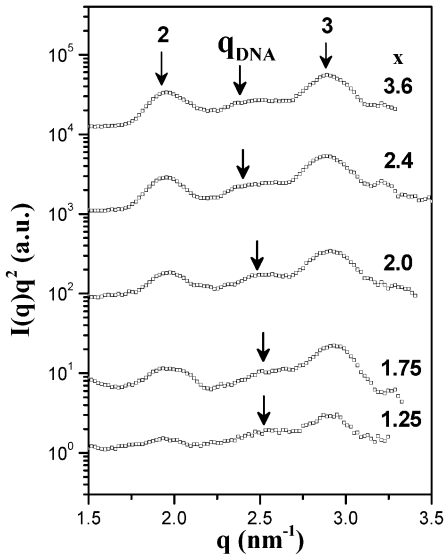

Figure 6. Enlarged plots of the SAXS profiles showing the presence of a DNA−DNA correlation peak at ca. 2.5 nm^{-1} (marked by the arrows) for DNA/DC-Chol complexes.

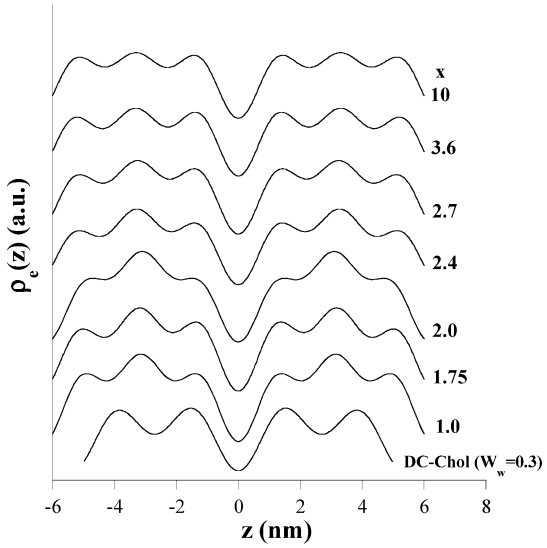

Figure 7. Relative electron density profiles of DNA/DC-Chol complexes in excess water. For $x = 10$ the corresponding $\rho_e(z)$ profile was obtained by subtracting the broad halo associated with unbound DC-Chol from the overall scattering profile.

structure in polymer systems (e.g., synthetic polymer/surfactant complexes in the bulk, block copolymers, and semicrystalline polymers). For DC-Chol with $W_w = 0.3$, the valley centered at $z = 0$ corresponds to the hydrophobic regions, while the two humps at $z \pm 1.53$ and $z \pm 3.84$ nm represent the headgroup regions. The water intercalated between the headgroups results in the shallow valley between the two humps. The thickness of the hydrophobic bilayer, approximately given by the headgroup-to-headgroup distance in the $\rho_e(z)$ profile, is ca. 3.0 nm for both neat DC-Chol and the complexes. The electron density profiles of the hydrophilic layers in the complexes are clearly different from the corresponding profile in DC-Chol. In contrast to a valley between two humps, a peak beside the humps is identified for the complexes irrespective of composition. This peak is attributed to the DNA sandwiched between the lipid headgroups. We also note that this peak is ca. 2.0 nm in width irrespective of composition, indicating

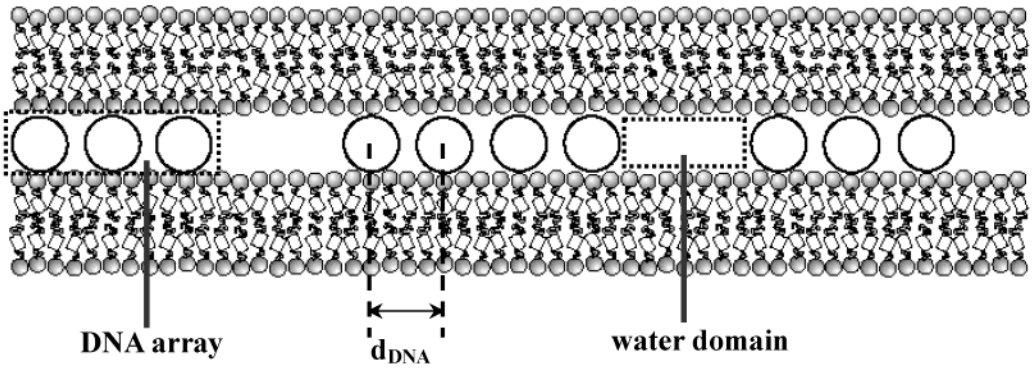

Figure 8. Schematic model showing the coexistence of closely packed DNA arrays and water domains in the hydrophilic layer for the complexes at $x > 2$.

that DNA duplex in the complexes adopts the common B conformation (diameter $\approx$ 2.0 nm).[40]

Although the electron density profiles are qualitatively similar among the complexes with different prescribed compositions, the electron density of the DNA peak in the hydrophilic layer (denoted by ρ_e^D) relative to that of the headgroup region (denoted by ρ_e^h) appears to decrease with increasing x as $x > 2$. ρ_e^D is obviously higher than ρ_e^h at $x \leq 2$, but they become approximately equal in height at $x \geq 3.6$. The composition-dependent ρ_e^D can be understood by considering that the excess unbound lipids coexist with the bound lipids within the lamellae (as supported by the TEM micrographs showing no cylindrical micelle formed by unbound DC-Chol molecules at $x \leq 3.6$). These unbound lipid molecules might be equally partitioned in the membrane; however, this would invariably swell the interhelical distance of the DNA chains in the hydrophilic layers. Since swelling of d_{DNA} is not observed (cf. Figure 6), the unbound lipid molecules must have segregated to form domains coexisting with the bound lipid domains within the lamellae, as schematically illustrated in Figure 8. In this case, the hydrophilic layers excluding the lipid headgroups contain domains of closely packed DNA arrays and water domains, and ρ_e^D would represent a harmonic average of the electron density of the DNA arrays and that of the water domains, where a lower ρ_e^D signifies a higher volume fraction of water domains in the hydrophilic layers. The intervention of the unbound lipid domains reduces the persistence length of the membrane due to the tendency toward micelle formation of unbound DC-Chol, and this may be responsible for the formation of circular lamellae at larger x (cf. Figure 5). Because of the absence of unbound lipid domains, flat lamellae are predominantly observed at $x < 2$ because the high packing density of DNA bound on the bilayer surface over a large distance increases the membrane rigidity.

Conclusions

The self-assembled structures of the binary complexes of polyanionic DNA with cationic DC-Chol lipid in the presence of excess water have been characterized by SAXS and TEM. DC-Chol lipids were found to form cylindrical micelles instead of bilayers in aqueous media. Complexation with DNA transformed the micelles into a multilamellar structure consisting of alternating lipid bilayer and DNA monolayer. Consequently, complexation with DNA induced both formation and ordering of DC-Chol bilayers because of the effective dehydration of the DC-Chol headgroups induced by the electrostatic interaction with DNA. The complexation was found to be a highly cooperative process, where the binding of DC-Chol molecules onto DNA proceeded through a zipper mechanism to yield nearly 1:1 stoichiometry for the complexes even when DNA was in excess of the lipid in terms of the overall ionic charge. Although not being able to represent the actual complex composition correctly, the prescribed composition given by the overall lipid-to-base pair molar ratio was a key variable governing the complex structures at different length scales. At $x \ll 2$, the DNA chains confined between the bilayers formed closely packed arrays (with the in-plane interhelical distance of 2.51 nm) over a large distance without the intervention of unbound lipid domains. The high packing density of DNA stiffened the membrane, thereby resulting in a topological structure of flat lamellae. When the lipid became in excess, the hydrophilic layers excluding the lipid headgroups contained domains of closely packed DNA arrays and water domains. In this case, the persistence length of the membrane was reduced by the intervention of unbound lipid domains, and this induced the formation of circular lamellae.

Acknowledgment. This work was supported by the National Science Council of R.O.C. under Grant NSC 91-2216-E-007-016.

References and Notes

(1) Zhou, S.; Chu, B. *Adv. Mater.* **2000**, *12*, 545.
(2) Antonietti, M.; Burger, C.; Effing, J. *Adv. Mater.* **1995**, *7*, 751.
(3) Ober, C. K.; Wegner, G. *Adv. Mater.* **1997**, *8*, 17.
(4) Rädler, J. O.; Koltover, I.; Salditt, T.; Safinya, C. R. *Science* **1997**, *275*, 810.
(5) Lasic, D. D.; Templeton, N. S. *Adv. Drug Delivery Rev.* **1996**, *20*, 221.
(6) Miller, A. D. *Angew. Chem. Int. Ed.* **1998**, *37*, 1768.
(7) Chesnoy, S.; Huang, L. *Annu. Rev. Biophys. Biomol. Struct.* **2000**, *29*, 27.
(8) Rädler, J. O.; Koltover, I.; Jamieson, A.; Salditt, T.; Safinya, C. R. *Langmuir* **1998**, *14*, 4272.
(9) Sternberg, B.; Sorgi, F. L.; Huang, L. *FEBS Lett.* **1994**, *356*, 361.
(10) Huang, L.; Hung, M. C.; Wagner, E. *Nonviral Vectors for Gene Therapy*; Academic Press: New York, 1999.
(11) Gustafsson, J.; Arvidson, G.; Karlsson, G.; Almgren, M. *Biochim. Biophys. Acta* **1995**, *1235*, 305.
(12) Pitard, B.; Aguerre, O.; Airiau, M.; Lachages, A. M.; Boukhnikachvili, T.; Byk, G.; Dubertret, C.; Herviou, C.; Scherman, D.; Mayaux, J. F.; Crouzet, J. *Proc. Natl. Acad. Sci. U.S.A.* **1997**, *94*, 14412.
(13) Lasic, D. D.; Strey, H.; Stuart, M. C. A.; Podgornik, R.; Frederik, P. M. *J. Am. Chem. Soc.* **1997**, *119*, 832.
(14) Koltover, I.; Salditt, T.; Safinya, C. R. *Biophys. J.* **1999**, *77*, 915.

(15) Koltover, I.; Salditt, T.; Rädler, J. O.; Safinya, C. R. *Science* **1998**, *281*, 78.
(16) Koltover, I.; Wagner, K.; Safinya, C. R. *Proc. Natl. Acad. Sci. U.S.A.* **2000**, *97*, 14046.
(17) Fang, Y.; Yang, J. *J. Phys. Chem. B* **1997**, *101*, 441.
(18) Fang, Y.; Yang, J. *J. Phys. Chem. B* **1997**, *101*, 3453.
(19) Malghani, M. S.; Yang, J. *J. Phys. Chem. B* **1998**, *102*, 8930.
(20) Fang, Y.; Hoh, J. H. *J. Am. Chem. Soc.* **1998**, *120*, 8903.
(21) Ono. M. Y.; Spain, E. M. *J. Am. Chem. Soc.* **1999**, *121*, 7330.
(22) Leonenko, Z. V.; Merkle, D.; Lees-Miller, S. P.; Cramb, D. T. *Langmuir* **2002**, *18*, 4873.
(23) Battersby, B. J.; Grimm, R.; Huebner, S.; Ceve, G. *Biochim. Biophys. Acta* **1998**, *1372*, 379.
(24) Huebner, S.; Battersby, B. J.; Grimm, R.; Cevc, G. *Biophys. J.* **1999**, *76*, 3158.
(25) Schmutz, M.; Durand, D.; Debin, A.; Palvadeau, Y.; Etienne, A.; Thierry, A. R. *Proc. Natl. Acad. Sci. U.S.A.* **1999**, *96*, 12293.
(26) Pitard, B.; Oudrhiri, N.; Vigneron, J. P.; Hauchecorne, M.; Aguerre, O.; Toury, R.; Airiau, M.; Ramasawmy, R.; Scherman, D.; Crouzet, J.; Lehn, J. M.; Lehn, P. *Proc. Natl. Acad. Sci. U.S.A.* **1999**, *96*, 2621.
(27) Raspaud, E.; Pitard, B.; Durand, D.; Aguerre-Chariol, O.; Pelta, J.; Byk, G.; Scherman, D.; Livolant, F. *J. Phys. Chem. B* **2001**, *105*, 5291.
(28) Zantl, R.; Baicu, L.; Artzner, F.; Sprenger, I.; Rapp, G.; Rädler, J. O. *J. Phys. Chem. B* **1999**, *103*, 10300.
(29) Liang, H.; Angelini, T. E.; Ho, J.; Braun, P. V.; Wong, G. C. L. *J. Am. Chem. Soc.* **2003**, *125*, 11786.
(30) Gao, X.; Huang, L. *Biochem. Biophys. Res. Commun.* **1991**, *179*, 280.
(31) Dias, R.; Mel'nikov, S.; Lindman, B.; Miguel, M. G. *Langmuir* **2000**, *16*, 9577.
(32) Medellin-Rodriguez, F. J.; Phillips, P. J.; Lin, J. S. *Macromolecules* **1996**, *29*, 7491.
(33) Liou, W.; Geuze, H. J.; Slot, J. W. *Histochem. Cell Biol.* **1996**, *106*, 4.
(34) Hayagawa, K.; Santerre, J. P.; Kwak, J. C. T. *Macromolecules* **1983**, *16*, 1642.
(35) Chandar, P.; Somasundaran, P.; Turro, N. J. *Macromolecules* **1988**, *21*, 950.
(36) Philips, B.; Dawydoff, W.; Linow, K. J. *Z. Chem.* **1982**, *22*, 1.
(37) Bakturov, E. A.; Bimendina, L. A. *Adv. Polym. Sci.* **1982**, *41*, 99.
(38) Kabanov, V. A.; Zezin, A. B. *Makromol. Chem. Suppl.* **1984**, *6*, 259.
(39) Jones, A. A. L. *Soft Condensed Matter*; Oxford University Press: New York, 2002.
(40) Podgornik, R.; Rau, D. C.; Parsegian, V. A. *Macromolecules* **1989**, *22*, 1780.
(41) Wachtel, E.; Borochov, N.; Bach, D.; Miller, I. R. *Chem. Phys. Lipids* **1998**, *92*, 127.
(42) Heller, W. T.; Waring, A. J.; Lehrer, R. I.; Harroun, T. A.; Weiss, T. M.; Yang, L.; Huang, H. W. *Biochemistry* **2000**, *39*, 139.
(43) Pott, T.; Roux, D. *FEBS Lett.* **2002**, *511*, 150.
(44) Lewis, R. N. A. H.; Winter, I.; Kriechbaum, M.; Lohner, K.; McElhaney, R. N. *Biophys. J.* **2001**, *80*, 1329.

MA049541P